

H α AS A TRACER OF MASS LOSS FROM OB STARS

CLAUS LEITHERER

Joint Institute for Laboratory Astrophysics, University of Colorado and National Bureau of Standards

Received 1987 July 10; accepted 1987 August 14

ABSTRACT

This paper investigates the use of the H α emission from stellar winds of OB stars to determine the stellar mass-loss rate. The power in H α emitted by the wind can be parameterized in terms of the temperature and the density field of the wind. A simple expression is derived which relates the observed H α luminosity to the stellar mass-loss rate, the stellar radius, the velocity law, and the stellar effective temperature. This expression is calibrated for the influence of the velocity law using a sample of Galactic OB stars with UV mass-loss rates. Consequently, the results depend on the validity of the UV rates. The derived velocity law for O stars turns out to be in agreement with the radiation–pressure-driven wind theory. There is evidence for a dependence of the velocity-law gradient on spectral type. The results for B stars, however, are more uncertain due to the dependence on the adopted \dot{M}/L relation. Application of the calibrated H α luminosity/mass-loss rate relation to a sample of 149 galactic OB stars shows that \dot{M} can be reliably determined from H α . Due to the moderate amount of observing time required to derive \dot{M} from H α , this method may be applied successfully to investigate mass-loss effects in extragalactic stars.

Subject headings: line profiles — stars: early-type — stars: mass loss

I. INTRODUCTION

Stellar winds play an important role in the evolution of hot, luminous stars. The effects of mass loss on the H-R diagram for massive stars have been discussed, e.g., by Maeder (1984).

The stellar mass-loss rate \dot{M} can be derived by several observational techniques. Each of these techniques basically measures a density at some place in the wind. Derivation of \dot{M} then requires the knowledge of the velocity field of the outflow. The flow starts at the stellar surface with an initial velocity of the order of the sound speed, is rapidly accelerated, and approaches a terminal velocity v_∞ of about 2–3 times the surface escape velocity at a distance of ~ 10 stellar radii. As the kinetic energy of the flow at this distance is much higher than the gravitational energy of the mass-losing star, v_∞ remains constant until the interaction with the interstellar medium at $\sim 10^4$ stellar radii decelerates the wind. Although this general picture is fairly well established, the detailed run of the velocity field in the acceleration zone within a few stellar radii is badly known.

The most versatile technique to derive \dot{M} makes use of resonance lines of highly ionized metals observable in the satellite UV. Due to a combination of atomic parameters and stellar-wind densities, these lines originate in those wind zones where the main acceleration has already been reached. Thus the line profiles allow one to derive the column density so that \dot{M} can be determined (see, e.g., Garmany *et al.* 1981).

Another method to obtain \dot{M} is based on the free-free emission detectable from the ionized stellar wind. Since the optical depth of the free-free emission increases with increasing wavelength, this technique samples the region beyond the UV zone if one observes at radio wavelengths or the region inside the UV zone close to the star if observations are performed in the infrared. Therefore radio measurements of \dot{M} when used in combination with the terminal-velocity information provided by the UV method are considered very reliable. In contrast, infrared photometry suffers heavily from the velocity informa-

tion which is not well known so close to the star. As a consequence, the IR method is usually regarded as an unreliable mass-loss tracer. Discussions of the radio and infrared methods can be found in Abbott (1985) and Abbott, Telesco, and Wolff (1984), respectively.

H α emission can be detected in many stellar winds. The H α -emitting region approximately coincides with the IR-emitting region implying a strong velocity field dependence for H α , too. In principle, high-resolution H α spectroscopy could yield density and velocity information to derive \dot{M} (Olson and Ebbets 1981). In practice, however, the required synthetic-line profile fitting is quite ambiguous so that this method could be applied for a few stars only. On the other hand, if we knew the velocity law, then H α would be fairly model-independent and could provide a reliable \dot{M} tracer. Model calculations performed by Klein and Castor (1978, hereafter KC) assuming a fixed velocity law predicted a tight relationship between the H α luminosity of the stellar wind and \dot{M} . Unfortunately, \dot{M} derived by this method has been considered to be systematically too high due to the velocity law adopted by KC (Lamers 1981).

In this paper we are reinvestigating the relationship between H α luminosity and mass loss. We are motivated by the increasing need for mass-loss rates of extragalactic stars. The theory of radiation–pressure-driven winds predicts significantly lower mass-loss rates in metal-poor galaxies (Abbott 1982; Kudritzki, Pauldrach, and Puls 1987). If this prediction can be proven by observations, profound implications for the evolution of massive stars, e.g., in the SMC or IC 1613, are expected. However, the apparent faintness of stars in these galaxies makes mass-loss determinations extremely difficult with any of the above \dot{M} tracers except with H α .

Section II describes the extension of the KC models for arbitrary velocity laws. In § III we empirically determine H α envelope luminosities for 149 OB stars. By calibrating the H α method using velocity-law-independent data we derive the

average velocity law for our sample of OB stars in § IV. In §§ V and VI we demonstrate the potential value of the H α method in determining \dot{M} for Galactic and extragalactic stars.

II. THEORETICAL H α LUMINOSITY OF THE STELLAR WIND

KC performed a set of statistical equilibrium calculations for hydrogen and ionized helium which allowed them to derive a numerical relation between the total power emitted by the stellar wind in H α and the mass-loss rate for a given velocity law of the outflow. Their results found for the electron temperature and the departure coefficients in the envelope can be used to extent their models to arbitrary velocity laws.

The power emitted by the stellar wind in H α , $L(\text{H}\alpha)$, can be related to the population density of the third level of hydrogen, N_3 , by

$$L(\text{H}\alpha) = \int w N_3 A_{32} h\nu_{32} dV. \quad (1)$$

In this equation, A_{32} is the transition probability for spontaneous emission for H α , $h\nu_{32}$ is the energy of an H α photon, and w corrects the volume integration for the solid angle subtended by the stellar core. The value of w is given by

$$w = \frac{1}{2} + \frac{1}{2} \left(1 - \left(\frac{R}{r} \right)^2 \right)^{1/2}, \quad (2)$$

where r/R is the distance from the stellar center in units of stellar radii. For H α work, w is only a small correction factor for the actual volume integration. Notice that equation (1) holds only if $\tau(\text{H}\alpha) \ll 1$, an assumption that is usually fulfilled in O stars but may break down for certain B stars (see § V).

N_3 in equation (1) can be expressed in terms of the electron density N_e and the proton density N_p using the NLTE-Saha

equation. One finds:

$$L(\text{H}\alpha) = \frac{9h^3 A_{32} h\nu_{32}}{(2\pi m_e k)^{3/2}} \int w N_e N_p b_3 T_e^{-3/2} \exp\left(\frac{17530}{T_e}\right) dV; \quad (3)$$

b_3 denotes the departure coefficient for the $n = 3$ level of hydrogen. The constants introduced by the Saha equation are self-explanatory. If we assume spherical symmetry (for the lack of observational evidence against it) and set $N_e = N_p$ we can make use of the equation of continuity to write:

$$L(\text{H}\alpha) = \frac{9h^3 A_{32} h\nu_{32}}{4\pi\mu^2 m_H^2 (2\pi m_e k)^{3/2}} \int w \frac{\dot{M}^2}{r^2 v(r)^2} b_3 T_e^{-3/2} \times \exp\left(\frac{17530}{T_e}\right) dr, \quad (4)$$

where $v(r)$ is the velocity field of the stellar wind, \dot{M} is the mass-loss rate, and μ is the average atomic weight.

KC's model calculations have shown that $b_3(r)$ and $T_e(r)$ can to a good approximation be written as $b_3 \approx 1.26$ and $T_e \approx 0.9 T_{\text{eff}}$. Under these assumptions we can easily calculate the temperature-dependent constant $c(T_{\text{eff}})$ defined as:

$$c(T_{\text{eff}}) = \log \left[b_3 T_e^{-3/2} \exp\left(\frac{17530}{T_e}\right) \right]. \quad (5)$$

The results are illustrated in Figure 1. The solid curve in this figure is the prediction of equation (5). The dots represent the actual values for $c(T_{\text{eff}})$ based on the KC model calculations where b_3 and T_e are obtained self-consistently from radiative equilibrium calculations and are *not* assumed to be constant throughout the envelope. The agreement is excellent. Since, from equation (4), $\log \dot{M}$ scales with $-0.5 c(T_{\text{eff}})$, it is safe to conclude that any \dot{M} determination via equation (4) will be

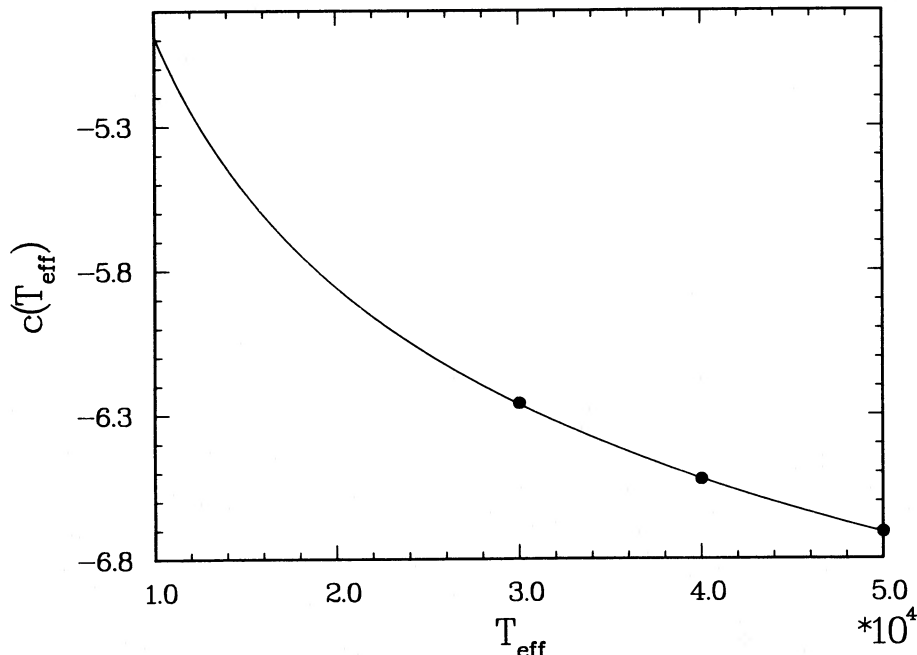


FIG. 1.—Calculated temperature dependence of $c(T_{\text{eff}})$ defined by eq. (5) (solid line). The three dots represent the results of the self-consistent calculations by KC.

only affected slightly by an error in $c(T_{\text{eff}})$. Even for B stars, we can expect b_3 to be of the order unity so that equation (4) can also be successfully applied if $T_{\text{eff}} < 30,000$ K [provided $\tau(\text{H}\alpha) \ll 1$ still holds].

The integration in equation (4) then has only to be performed over the quantity $w/[rv(r)]^2$. The velocity law is parameterized in a way proposed by Castor and Lamers (1979):

$$v(r) = v_0 + (v_\infty - v_0) \left(1 - \frac{R}{r}\right)^\beta. \quad (6)$$

With this parameterization the flow starts at an initial velocity v_0 on the stellar surface and asymptotically reaches the terminal velocity v_∞ further out. The exponent β governs the "slope" of $v(r)$. A graph of $v(r)$ for different values of β can be found, e.g. in Bertout *et al.* (1985).

The integral in equation (4) can be rewritten by means of the substitutions $u = v_0/v_\infty$ and $x = R/r$ so that

$$\int \frac{w}{r^2 v(r)^2} dr = \frac{1}{R v_\infty^2} \int_0^1 \frac{(1/2) + [1/2(1-x^2)^{1/2}]}{[u + (1-u)(1-x)^\beta]^2} dx. \quad (7)$$

Figure 2 gives the numerical values for the logarithm of the integral on the right-hand side of equation (7) (denoted by I). It is obvious from this figure that $L(\text{H}\alpha)$ is critically dependent on the appropriate choice of the velocity law. If, e.g., β is varied from 0.5 to 0.7 \dot{M} correspondingly scales by about a factor of 2. This figure also emphasizes the role of the initial velocity v_0 . As long as $\beta < 1$, the flow velocity increases so rapidly that the velocity of the $\text{H}\alpha$ emitting region is well above v_0 and the actual value of v_0 hardly affects I . On the other hand, for larger values of β we have $v(r) \approx v_0$ in an appreciable part of the envelope and I will critically depend on v_0 .

Using equations (5) and (7) together with the appropriate values for the numerical constants we find for the $\text{H}\alpha$ luminosity of the envelope:

osity of the envelope:

$$\log L(\text{H}\alpha) = 2 \log |\dot{M}| - 2 \log v_\infty - \log R + c(T_{\text{eff}}) + I + 25.125 \quad (8)$$

[$L(\text{H}\alpha)$ in L_\odot , \dot{M} in $M_\odot \text{ yr}^{-1}$, v_∞ in km s^{-1} , R in R_\odot]. Values of $c(T_{\text{eff}})$ and I are the quantities plotted in Figures 1 and 2, respectively. Equation (8) is an extension of the KC models for arbitrary velocity fields. In fact, this equation can be reduced to the three relations published by KC (their eqs. [22], [23], [24]) if their velocity law is used and their stellar parameters are inserted in equation (8). Since KC adopted a velocity law which becomes indefinite at $r = R$, the $v(r)$ integration is performed until $\tau(\text{H}\alpha) = 1$. With these conditions equation (8) is equivalent to the KC results.¹

From an observational point of view, the $L(\text{H}\alpha)$ versus \dot{M} relation given in the present paper is superior to the KC parameterization since we make use of R and v_∞ in contrast to the stellar mass M introduced by KC. The latter quantity is more difficult to determine observationally whereas R and v_∞ can be readily obtained from spectroscopy. Equation (8) then provides a very convenient means of investigating the stellar mass-loss rate in combination with the velocity law if $L(\text{H}\alpha)$ is known. $L(\text{H}\alpha)$ itself is simply related to the observed $\text{H}\alpha$ equivalent width $W(\text{H}\alpha)$.

III. $\text{H}\alpha$ ENVELOPE LUMINOSITIES OBSERVED IN OB STARS

Observations of $\text{H}\alpha$ profiles in early-type stars have been reported in a variety of papers. We searched through the liter-

¹ In eq. (19) of KC, the statistical weight factor has been omitted. Furthermore, eq. (20) is not the original CAK velocity law. The actual calculations of KC, however, had been done with the correct statistical weight and the CAK velocity law (J. I. Castor, private communication).

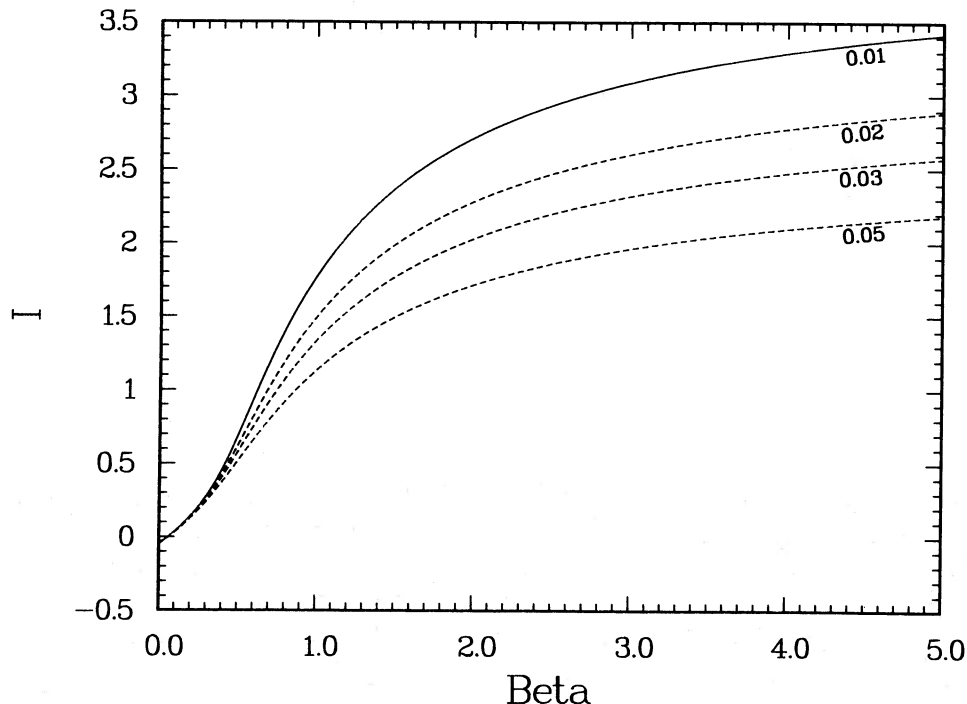


FIG. 2.—Influence of the velocity law exponent β on the logarithm of the integral in eq. (7). The four curves have been calculated with $v_0/v_\infty = 0.01, 0.02, 0.03,$ and 0.05 .

ature to find published $H\alpha$ equivalent widths for as many OB stars as possible. The following selection criteria have been applied:

1. The program stars should be of spectral type O and B. Stars of later spectral types have less dense winds and/or stronger photospheric $H\alpha$ absorption so that the $H\alpha$ envelope emission becomes essentially undetectable.

2. Known binaries have been excluded. This avoids mass-loss rates that may be affected by binary interaction. Moreover, the observed stellar luminosity would be influenced by the presence of a companion.

3. The program stars should have a reliable M_v determination, either by spectral classification or—preferentially—by cluster membership. In fact, 84% of the program stars are confirmed members of open clusters or OB associations.

The outcome of the literature survey are $H\alpha$ equivalent widths for 149 OB stars. The sources are Abbott, Biegging, and Churchwell (1981), Conti (1974), Conti and Frost (1977), Ebbets (1982), Peppel (1984), Rosendhal (1973), and Sterken and Wolf (1978). In those cases where $W(H\alpha)$ of one star was measured independently by several authors, we simply took an unweighted mean of the individual values. This may not be entirely satisfactory, but it is hard to judge between older photographic measurements or determinations based on Reticon detectors. Although at first glance the second method seems to deserve greater weight, observations performed with Reticon detectors often suffer from the limited free spectral range. Since many OB stars possess very broad $H\alpha$ profiles with wings extending up to $\approx \pm 1000 \text{ km s}^{-1}$ so that the continuum determination becomes crucial, the Reticon data may not necessarily be superior to photographic data. In fact the differences in $W(H\alpha)$ of one star determined by Reticon and photographic observations are of the same magnitude as differences in $W(H\alpha)$ published by two different authors both using photographic plates. Part of these differences may be due to real

variations of the $H\alpha$ profiles as has been demonstrated by Ebbets (1982). These variations can amount up to a factor of 2 in $W(H\alpha)$ in certain cases. Consequently, the quantities derived from $W(H\alpha)$ using equation (8) will also show this range of variation. The $H\alpha$ equivalent widths finally adopted are listed in the third column of Table 1.

Figure 3 is a histogram illustrating the distribution of the selected program stars over spectral type. Most spectral types are well represented, especially stars of spectral type B1 and earlier. In the case of the O stars, all luminosity classes are covered. The B stars show traceable $H\alpha$ emission only if M_v is high enough so that the inclusion of nonsupergiant B stars would yield no further insight into the present problem.

The conversion of $W(H\alpha)$ (\AA) into $L(H\alpha)$ (ergs s^{-1}) is done following standard procedures as described, e.g., by Conti and Frost (1977). The spectral classifications and M_v values are adopted mostly from the compilation of Humphreys (1978). For stars with no M_v based on cluster membership we use the spectral type/ M_v calibration given by Schmidt-Kaler (1982). This source also provides the T_{eff} , and bolometric correction scale. These quantities allow one to locate the stars in the Hertzsprung-Russell diagram. Comparison with theoretical evolutionary tracks with mass loss (Maeder 1984) then yields the stellar mass (the fourth column of Table 1) so that $\log g$ can be obtained. T_{eff} and $\log g$ are used to assign a photospheric $H\alpha$ absorption profile to each star, which is subtracted from the observed profile. The photospheric profiles are taken from Auer and Mihalas (1972), for $50,000 \text{ K} > T_{\text{eff}} \leq 30,000 \text{ K}$, from Mihalas (1972) for $30,000 \text{ K} > T_{\text{eff}} \geq 15,000 \text{ K}$, and from Kurucz (1979) for $15,000 \text{ K} > T_{\text{eff}} > 10,000 \text{ K}$. In the case of $T_{\text{eff}} \geq 15,000 \text{ K}$ we use NLTE profiles, whereas for $T_{\text{eff}} < 15,000 \text{ K}$ only LTE profiles are available. However, as can be recognized from the comparison in Mihalas (1972), if $T_{\text{eff}} \approx 20,000 \text{ K}$ then there is hardly a difference between LTE and NLTE profiles for luminosity classes V through Ia.

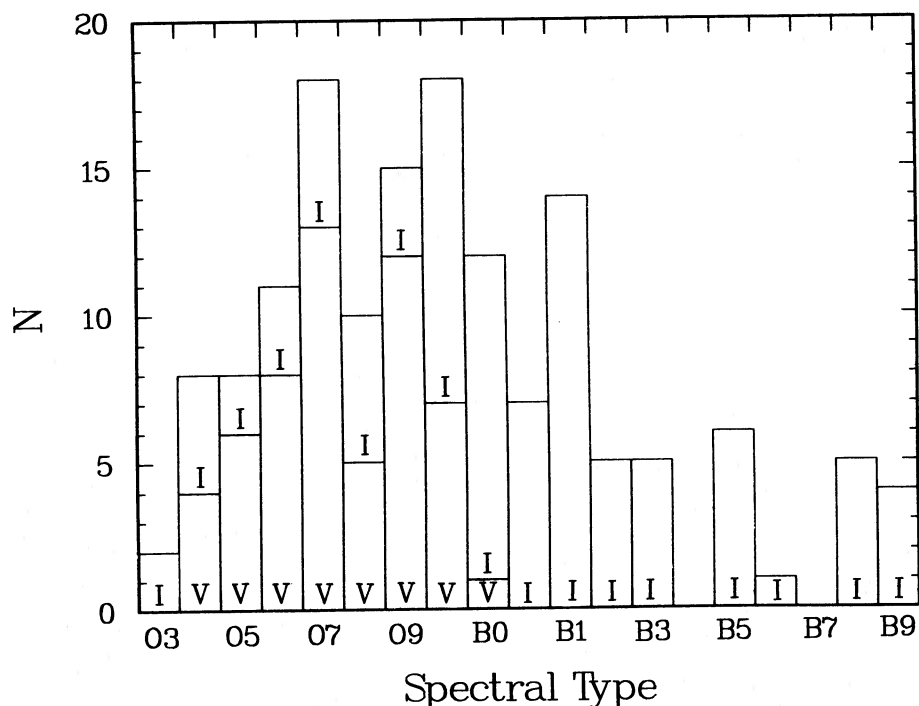


FIG. 3.—Histogram showing the distribution of the program stars vs. spectral type. *I* denotes luminosity classes I and II and *V* denotes classes III, IV, and V.

TABLE 1
ADOPTED AND DERIVED DATA FOR THE PROGRAM STARS

Object	Spectral Type	$W(\text{H}\alpha)$ (Å)	M/M_{\odot}	$\log[L(\text{H}\alpha)/L_{\odot}]$	$\log(L/L_{\odot})$	R/R_{\odot}	v_{∞} (km s^{-1})	I	$\log[M(M_{\odot} \text{ yr}^{-1})]$	$\log[\tau(\text{H}\alpha)]$
HD 108	O6f	-12.3	55	1.37	5.86	18	3900	2.16	-4.94	-2.1
HD 2905	B1Ia	- 2.1	35	1.19	5.50	43	1650	2.16	-5.90	-2.3
HD 4841	B5Ia	- 0.3	15	1.16	5.18	69	450+	1.73	-6.77	-1.1
HD 5005	O6.5V((f))	+ 2.4	50	-0.60	5.58	13	2650+	0.60	-6.18	-3.2
HD 5551	B1.5Ib	- 0.5	20	0.78	5.30	39	1100+	1.92	-6.36	-2.0
HD 12301	B8Ib	+ 1.9	10	0.31	4.26	35	500+	3.40	-7.54	-2.1
HD 12323	ON9V	+ 2.6	15	-1.73	4.62	6	1900+	1.83	-7.22	-3.7
HD 12993	O6.5V	+ 2.3	30	-0.87	5.18	8	2500	1.39	-6.44	-3.3
HD 13267	B5Ia	+ 0.8	15	0.74	4.98	55	500+	1.95	-6.99	-1.2
HD 13268	O7	+ 1.8	35	-0.26	5.38	11	2300	1.36	-6.14	-2.9
HD 13402	B05Ib	+ 0.3	25	0.54	5.30	27	1800+	2.14	-6.16	-2.4
HD 13745	O9.7II	+ 1.0	25	-0.17	5.22	15	2400	1.93	-6.29	-3.1
HD 14134	B3Ia	\pm 0.0	20	0.85	5.26	54	550+	1.47	-6.71	-1.8
HD 14818	B2Ia	+ 0.1	20	0.70	5.34	46	800+	1.47	-6.54	-2.2
HD 14947	O5If	- 6.4	70	1.15	5.90	18	2700	1.50	-5.16	-2.1
HD 14956	B2Ia	+ 0.2	25	0.77	5.34	46	900+	1.65	-6.45	-2.2
HD 15497	B6Ia	+ 0.7	15	1.08	5.22	79	400+	1.45	-6.88	-1.5
HD 15558	O5III	+ 1.2	85	0.48	6.06	19	3000	0.48	-5.41	-2.5
HD 15570	O4If	- 9.8	100	1.53	6.26	23	2700	0.90	-4.85	-1.7
HD 15629	O5V	+ 1.9	60	-0.11	5.86	14	3250	0.51	-5.73	-2.9
HD 16429	O9.5II	+ 0.8	50	0.51	5.82	30	2400+	0.97	-5.77	-2.8
HD 16691	O4If	- 6.6	70	0.96	5.82	14	3450+	1.74	-5.14	-2.2
HD 18326	O7V	+ 2.1	30	-0.68	5.10	8	2500+	1.81	-6.38	-3.2
HD 21291	B9Ia	+ 0.8	15	1.12	4.90	87	400+	2.21	-7.12	-0.8
HD 24398	B1Ib	+ 1.7	20	-1.46	5.14	28	1500	0.40	-7.36	-3.6
HD 24431	O9III	+ 2.1	25	-0.73	5.30	14	2050+	1.01	-6.51	-3.4
HD 24912	O7.5III	+ 1.4	35	-0.13	5.34	12	2500	1.70	-6.06	-3.0
HD 30614	O9.5Ia	- 1.9	45	1.03	5.74	30	1750	1.44	-5.66	-2.2
HD 34078	O9.5V	+ 3.2	25	< -0.94	5.18	13	800	< 0.31	< -7.13	< -2.9
HD 34085	B8Ia	+ 0.4	25	1.53	5.54	155	500	1.18	-6.57	-1.8
HD 34656	O7IIIf	+ 1.9	25	-0.47	5.26	10	2150+	1.42	-6.31	-3.0
HD 35600	B9Ib	+ 3.3	10	0.22	4.30	44	450+	3.07	-7.67	-1.9
HD 35619	O7V	+ 2.1	50	-0.22	5.62	15	2350	0.78	-6.05	-2.9
HD 36371	B5Iab	+ 0.9	15	0.88	5.14	66	450+	1.56	-6.92	-0.4
HD 36861	O8III	+ 3.2	35	< -0.86	5.34	13	2300	< 0.88	< -6.48	< -3.5
HD 37022	O7Vp	- 1.3	30	0.17	5.18	9	1650	2.09	-6.12	-2.0
HD 37041	O9V	+ 3.2	25	< -1.34	4.82	8	1650	< 1.54	< -7.03	< -3.4
HD 37043	O9III	+ 2.3	30	< -0.58	5.50	18	2400	< 0.75	< -6.32	< -3.4
HD 37128	B0Ia	- 0.1	45	0.86	5.70	35	2100	1.52	-5.76	-2.6
HD 37468	O9.5V	+ 2.6	25	< -0.98	5.14	13	2150+	< 1.23	< -6.73	< -3.7
HD 37737	O9.5III	+ 1.8	20	-0.70	4.86	9	1800+	2.15	-6.74	-2.8
HD 37742	O9.7Ib	- 0.1	50	0.87	5.82	35	2200	1.25	-5.66	-2.6
HD 38666	O9.5V	+ 3.9	15	< -1.58	4.54	6	2000	< 2.23	< -7.22	< -3.4
HD 38771	B0.5Ia	+ 0.6	30	0.64	5.46	34	1900	1.86	-6.04	-2.8
HD 40111	B0Ib	+ 1.0	30	0.28	5.46	26	1500	1.31	-6.24	-2.7
HD 41117	B2Ia	- 1.6	25	1.21	5.58	60	900	1.43	-6.17	-2.0
HD 42087	B2.5Ib	+ 0.5	20	0.26	4.98	35	700+	1.84	-6.95	-1.9
HD 42088	O6.5V	+ 2.4	35	-0.73	5.22	9	2550	1.43	-6.35	-3.3
HD 43384	B3Iab	+ 0.7	20	0.42	4.98	39	650+	1.94	-6.92	-1.7
HD 46149	O.85V	+ 3.4	25	< -1.02	5.18	11	1700	< 0.93	< -6.75	< -3.3
HD 46150	O5V	+ 3.3	60	< -0.71	5.86	14	3250	< -0.10	< -6.03	< -3.4
HD 46202	O9V	+ 2.8	25	< -1.26	4.90	9	2100+	< 1.60	< -6.87	< -3.6
HD 46223	O4V	+ 1.9	70	-0.17	5.82	12	3100	0.51	-5.75	-2.7
HD 46485	O7V	+ 3.0	30	< -1.10	5.22	9	2350+	< 0.99	< -6.59	< -3.5
HD 46966	O8V	+ 2.6	25	-2.10	5.22	10	2300	-0.04	-7.14	-4.4
HD 47839	O7V	+ 2.8	30	< -1.02	5.30	10	3100	< 1.09	< -6.40	< -3.6
HD 53138	B3Ia	+ 0.5	20	0.54	5.02	41	600	1.85	-6.90	-1.5
HD 57061	O9II	+ 1.3	50	0.42	5.98	30	2300	0.40	-5.72	-2.7
HD 57682	O9V	+ 1.9	30	-1.06	5.42	15	1700	0.20	-6.73	-3.5
HD 58350	B5Ia	\pm 0.0	20	1.05	5.14	66	550	1.90	-6.75	-1.4

TABLE 1—Continued

Object	Spectral Type	$W(H\alpha)$ (Å)	M/M_{\odot}	$\log[L(H\alpha)/L_{\odot}]$	$\log(L/L_{\odot})$	R/R_{\odot}	(km s^{-1})	I	$\log[M(M_{\odot} \text{ yr}^{-1})]$	$\log[\tau(H\alpha)]$
HD 66811	O4f	- 3.6	60	1.02	6.02	17	2650	1.03	-5.18	-2.0
HD 93129A	O3If	- 8.1	130	1.59	6.46	25	3900	0.71	-4.59	-1.8
HD 149038	B0Ia	+ 0.8	40	0.57	5.66	33	2200	1.38	-5.89	-2.9
HD 149438	B0V	+ 2.5	15	-1.58	4.50	7	2000	2.33	-7.30	-3.3
HD 151804	O8Iaf	-13.2	70	1.87	6.14	33	2000	1.29	-4.98	-1.6
HD 152233	O6IIIIf	+ 1.4	55	0.30	5.90	19	3250	0.80	-5.55	-2.8
HD 152236	B1.5Ia ⁺	- 6.5	50	2.11	6.06	98	400	0.29	--	+1.6
HD 152249	OC9.5Iab	+ 0.1	35	0.58	5.54	23	2200	1.74	-5.84	-2.7
HD 152408	O8Iafpe	-34.7	70	2.12	6.06	30	1800	1.68	-4.91	-1.3
HD 152424	OC9.7Ia	- 0.6	50	1.01	5.82	35	2250	1.41	-5.59	-2.5
HD 154090	B1Iabe	- 0.7	25	0.70	5.22	31	1100+	2.08	-6.39	-1.9
HD 158408	B3Ib	+ 3.1	15	< -0.71	4.62	26	700+	< 1.87	< -7.54	< -2.7
HD 162978	O8.5IIIIf	+ 1.6	35	-0.22	5.50	17	2700+	1.21	-6.08	-3.2
HD 163800	O7III	+ 2.2	55	-0.60	5.70	17	2750+	0.32	-6.15	-3.3
HD 164353	B5Ib	+ 1.9	10	-0.22	4.38	28	500	2.65	-7.61	-1.8
HD 164402	B0Ib	+ 1.6	25	-0.32	5.30	22	2000+	1.38	-6.47	-3.4
HD 164492	O7.5IIII	+ 2.8	40	< -0.82	5.42	13	3250+	< 1.00	< -6.28	< -3.6
HD 164794	O4V	+ 2.1	85	0.04	6.10	16	3450	0.06	-5.52	-2.8
HD 167263	O9.5II-III	+ 2.2	45	< -0.46	5.58	23	1800	< 0.41	< -6.43	< -3.2
HD 167264	B0Ia	+ 0.6	45	0.58	5.62	32	1900	1.38	-5.96	-2.7
HD 167659	O7II	+ 1.9	50	-0.16	5.78	20	2550	0.49	-5.94	-3.0
HD 167771	O7If	+ 0.8	50	0.49	5.86	22	2800+	0.99	-5.56	-2.7
HD 167971	O8Ibf	- 5.0	50	1.27	5.90	25	3100	1.73	-5.15	-2.3
HD 168075	O6.5IIII	+ 7.1	45	< -0.86	5.46	12	2650+	< 0.66	< -6.34	< -3.4
HD 168076	O4V	- 2.6	80	0.77	5.98	14	3700+	1.17	-5.16	-2.3
HD 168112	O5IIII	+ 2.0	70	0.06	5.90	16	3250	0.56	-5.61	-2.8
HD 169454	B1Ia ⁺	- 9.4	45	1.99	5.86	65	1300+	1.76	--	+0.1
HD 186745	B8Ia	- 0.3	15	1.36	5.26	112	350+	1.39	-6.92	-1.3
HD 186841	B1Ia	- 0.2	20	0.73	5.34	35	1400+	1.97	-6.26	-2.3
HD 188001	O8If	- 3.0	50	1.07	5.86	24	2300	1.39	-5.39	-2.3
HD 188209	O9.5I	- 1.2	45	0.82	5.62	26	2100	1.72	-5.72	-2.5
HD 190429A	O4If ⁺	- 7.9	90	1.31	6.10	19	3400+	1.32	-4.90	-2.0
HD 190429B	O9.5IIII	+ 1.4	25	-0.37	5.26	15	2400+	1.63	-6.35	-3.3
HD 190603	B1.5Ia ⁺	- 3.0	30	1.40	5.58	56	1000	1.70	--	-0.1
HD 190864	O6.5IIII	+ 1.8	45	-0.06	5.62	15	2950	1.14	-5.85	-3.0
HD 190918	B1Ib	+ 1.0	20	0.22	4.98	23	1700+	2.63	-6.51	-1.9
HD 190919	B1Ib	+ 1.3	20	0.12	4.98	23	1700+	2.52	-6.56	-2.2
HD 191423	O9IIII	+ 2.1	25	-1.16	5.10	13	2550+	1.40	-6.65	-3.9
HD 192281	O5Vnp	+ 2.2	70	-0.25	5.94	15	3300+	0.14	-5.77	-3.1
HD 192422	B0.5Ib	- 0.3	25	0.71	5.34	30	1700+	2.16	-6.09	-2.3
HD 192639	O7Ibf	- 1.2	50	0.78	5.78	20	2950+	1.54	-5.41	-2.6
HD 192660	B0Ia	± 0.0	50	0.83	5.70	35	2250+	1.56	-5.74	-2.7
HD 193183	B1.5Ib	+ 0.7	15	0.08	5.06	31	850+	1.68	-6.87	-1.5
HD 193237	B1Ia ⁺	- 54.2	50	2.86	6.02	78	400	1.17	--	+1.6
HD 193322	O8.5IIII	+ 3.0	35	< -0.66	5.50	17	1800	< 0.43	< -6.47	< -3.2
HD 193514	O7Ibf	+ 0.5	50	0.50	5.78	20	2950+	1.26	-5.55	-2.7
HD 193682	O5	+ 1.3	55	0.06	5.82	13	3100+	0.74	-5.58	-2.5
HD 194839	B0.5Ia	- 1.1	30	0.86	5.42	32	1800+	2.14	-5.97	-2.2
HD 195592	O9.5I	- 4.7	45	1.28	5.74	30	2300+	1.93	-5.42	-2.2
HD 198478	B3Ia	- 0.1	15	0.61	4.94	37	600+	2.16	-6.88	-1.0
HD 199478	B8Ia	- 0.6	15	1.21	5.02	85	400+	2.02	-6.99	-0.6
HD 201345	ON9.5V	+ 2.6	20	-1.72	4.86	9	1850+	1.16	-7.23	-3.9
HD 202850	B9Iab	+ 1.1	10	0.80	4.54	58	400+	2.89	-7.37	-1.4
HD 204172	B0Ib	+ 0.7	25	0.27	5.34	23	1900	1.84	-6.18	-2.9
HD 205196	B0Ib	- 1.1	20	0.24	4.78	12	1600+	3.18	-6.42	-1.8
HD 206165	B2Ib	+ 1.1	15	0.63	5.06	33	850+	2.19	-6.63	-1.4
HD 207198	O9Ib-II	+ 1.6	30	-0.21	5.38	15	2650+	1.53	-6.13	-3.2
HD 207538	O9.5V	+ 2.7	25	-2.59	4.86	9	2100+	0.39	-7.62	-4.6
HD 208501	B8Ib	+ 1.0	10	0.68	4.62	54	400+	2.60	-7.35	-1.3
HD 209975	O9.5Ib	+ 1.2	25	-0.42	5.30	18	2300	1.43	-6.38	-3.4

TABLE 1—Continued

Object	Spectral Type	$W(H\alpha)$ (Å)	M/M_{\odot}	$\log[L(H\alpha)/L_{\odot}]$	$\log(L/L_{\odot})$	R/R_{\odot}	v_{∞} (km s ⁻¹)	I	$\log[\dot{M}(M_{\odot} \text{ yr}^{-1})]$	$\log[\tau(H\alpha)]$
HD 210839	O6I	- 1.3	60	0.84	5.90	19	2500	1.13	-5.39	-2.3
HD 212593	B9Iab	+ 2.3	10	0.69	4.58	60	400+	2.63	-7.44	-1.3
HD 213087	B0.5Ib	+ 0.6	20	0.33	5.18	25	1650+	2.21	-6.33	-2.4
HD 214680	O9V	+ 2.9	25	< -1.18	4.98	9	2000	< 1.42	< -6.83	< -3.6
HD 216532	O9.5V	+ 2.8	20	< -1.42	4.70	7	2050+	< 1.98	< -7.08	< -3.5
HD 216898	O9V	+ 2.8	20	< -1.38	4.66	7	2200+	< 2.18	< -6.97	< -3.3
HD 217086	O7V	+ 1.8	30	-0.39	5.34	11	2300+	1.36	-6.21	-3.0
HD 218915	O9.5I	+ 0.8	45	0.27	5.62	26	2400	1.29	-5.94	-3.0
HD 224424	B1Iab	- 1.0	25	0.91	5.38	37	1500+	2.11	-6.12	-2.1
HD 225146	O9.7Ib	+ 0.5	20	0.07	5.14	16	2100+	2.27	-6.26	-2.8
HDE227634	B0Ib	+ 1.8	60	-1.13	5.06	17	1700+	1.10	-7.00	-3.7
HDE228712	B0.5Ia	- 1.7	45	1.23	5.70	45	1850+	1.79	-5.70	-2.4
HDE242908	O4V	+ 1.1	20	0.12	5.82	12	3250	0.85	-5.59	-2.6
BD+60° 493	B0.5Ia	- 2.3	25	0.93	5.34	30	1700+	2.39	-5.98	-1.9
BD+60° 498	O9.5V	+ 3.0	25	< -1.22	4.90	9	2050+	< 1.62	< -6.93	< -3.5
BD+60° 501	O7V	+ 2.5	30	-0.83	5.14	9	2550	1.56	-6.43	-3.4
BD+60° 512	O7.5	+ 2.2	25	-0.91	5.26	10	2150+	0.99	-6.55	-3.3
BD+60° 594	O9V	+ 2.3	25	-1.16	4.98	9	2000+	1.44	-6.82	-3.5
BD-14° 5037	B1.5Ia	- 7.4	30	1.74	5.62	59	1100+	2.02	-5.80	-1.3
BD+22° 3782	O7V	+ 2.1	40	-0.41	5.50	13	2700+	1.03	-6.12	-3.1
BD+23° 3759	B0II	+ 1.8	30	-0.88	5.38	21	2250+	0.71	-6.67	-3.7
BD+23° 3761	B0II	+ 3.3	25	< -0.70	5.26	18	2200+	< 1.21	< -6.62	< -3.6
BD+24° 3866	O8f	- 2.0	45	0.94	5.82	23	2550+	1.46	-5.41	-2.4
BD+24° 3881	O6f	+ 1.3	50	0.06	5.62	13	2700+	1.19	-5.82	-2.7
BD+60° 2522	O6.5	+ 0.9	50	0.22	5.66	14	2550+	1.19	-5.76	-2.6
Cyg OB2 #7	O3If	-0.8	90	0.75	6.10	17	3650+	0.81	-5.12	-2.3
Cyg OB2 #8A	O6Ib	-0.5	100	1.10	6.26	30	3400+	0.67	-5.04	-2.3
Cyg OB2 #9	O5If	- 7.1	110	1.67	6.38	32	2900+	0.76	-4.75	-1.8
Cyg OB2 #12	B5Ia ⁺	- 5.1	45	2.56	6.26	240	1400	-	-	-

NOTE.—Stellar parameters of HD 167971 refer to the primary component of this multiple system (see Leitherer *et al.* 1987).

The $H\alpha$ equivalent widths thus corrected for photospheric absorption are then converted to absolute units using the observed stellar luminosity in the visual passband and the theoretical stellar energy distribution computed by Kurucz (1979). The results can be found in the fifth column of Table 1.

The most disturbing aspect inherent in deriving $L(H\alpha)$ is the method of accounting for the underlying photospheric absorption profile. The procedure of simply *subtracting* the photospheric contribution is not very sophisticated and assumes the photosphere and the stellar wind are separate entities, which is certainly not true. Clearly, a self-consistent method would be desirable which accounts for the influence of the stellar wind on the photospheric profile. Such models are not available to date. For the O stars, however, the photospheric profile is fairly insensitive to the actual choice of $\log g$ and T_{eff} . Additionally, in many cases the photospheric absorption profile is only a small correction to the emission profile of the stellar wind. Consequently, the derived $L(H\alpha)$ values are reliable for O stars. On the other hand, one should be aware that for B stars the photospheric absorption profile is sensitive to $\log g$ and additionally involves a *large* correction for the wind profile. Therefore $L(H\alpha)$ for mid- and late-B stars is much more uncertain than for stars of earlier spectral type.

IV. THE VELOCITY LAW

The $H\alpha$ envelope luminosities derived in the previous section can be used to obtain information on the density field of the

$H\alpha$ emitting region. The uncertain knowledge of $v(r)$ prevents us from determining \dot{M} via equation (8). On the other hand, we can use equation (8) to investigate $v(r)$ if we know \dot{M} . Ideally, we should like to have \dot{M} for all program stars determined by a $v(r)$ -independent method, e.g., by UV or radio techniques. However, less than 20% of the program stars have been observed with these techniques so that we cannot expect to have a statistically significant sample of calibrators.

On the other hand, radio and UV data reveal a tight correlation between \dot{M} and the stellar luminosity. Garmany and Conti (1984) find

$$\log \dot{M} = -6.87 + 1.62 \log L/10^5 \quad (9)$$

(\dot{M} in $M_{\odot} \text{ yr}^{-1}$, L in L_{\odot}). This relation holds over several orders of magnitude in \dot{M} and L . While there might be a dependence of \dot{M} on stellar parameters other than L , such correlations, if present, are too weak to be detectable given the observational uncertainties. Since a dependence of \dot{M} on L is also the prediction of the theory of radiation-pressure-driven winds, we adopt equation (9) to predict the average mass-loss rates for the program stars. We mention that equation (9) was originally derived from a sample of O stars. When we apply this relation to B stars we have to assume that we may extrapolate equation (9) toward lower effective temperatures. This assumption is supported by the wind theory which predicts no breakdown of the \dot{M}/L relation for B stars. Further observa-

tional support comes from a few \dot{M}/L data points for B stars published by Abbott (1985).

Using equation (9) we derive the average mass-loss rate for each star from its luminosity. We emphasize that this equation underestimates the mass loss for hypergiants. Since we have to exclude those stars from our sample for other reasons (see § V) we do not try to correct equation (9) to apply it to hypergiants. The stellar luminosity is listed in the sixth column of Table 1. The seventh column of this table gives the stellar radius as obtained from T_{eff} and L .

The terminal velocities of the stellar winds are tabulated in the eighth column of Table 1. For roughly one-third of the sample stars we found v_{∞} values based on UV observations published in the literature. The sources are Abbott (1978), Burki and Llorente de Andrés (1979), Burki *et al.* (1982), Conti (1988), Conti and Garmany (1980), Garmany and Conti (1984, 1985), Gathier, Lamers, and Snow (1981), Hutchings and von Rudloff (1980), and Leitherer *et al.* (1987). As in the case of \dot{M} we gave equal weights when averaging v_{∞} values published by different authors.

For those stars with no published terminal velocity, v_{∞} has been calculated from the surface escape velocity assuming $v_{\infty} = \text{constant } v_{\text{esc}}$. The constant depends on the stellar position in the HRD (Garmany and Conti 1984) with typical values being 3 for O stars and 1.5 for B stars. Terminal velocities thus derived are denoted by (+) in Table 1. They are less reliable than the values directly determined from observations. However, as compared with the uncertainty introduced by \dot{M} they are a minor source of error.

The ninth column of Table 1 lists the values for I derived via equation (8). We emphasize that I is to be interpreted in a statistical way since we make use of the statistical mass-loss rate. The standard deviation difference of $\log \dot{M}$ from equation (9) and the actual observed mass-loss rate is 0.48 (Garmany and Conti 1984) so that I has at least twice this standard

deviation for an individual star. Clearly, any positive correlation of I with some stellar parameter will show up only if we average over a large enough subset of stars all having equal values for a certain stellar parameter. After averaging over such a subset we may hope that the rms value of I is smaller than the variation of I from one subset to another, e.g., having different effective temperature. (This assumes there exists a correlation of the velocity law with some stellar parameter.)

The best correlation found is a dependence of I on the effective temperature. Since no $\log g$ dependence of I could be detected for the O stars, we averaged I over all luminosity classes of a given spectral type. Figure 4 shows the derived mean values of I as a function of spectral type. The error bars in this figure denote the rms values for the average I at a given spectral type. The dashed line in Figure 4 is an eyesight fit to the data points. Despite the scatter of the data, the trend for I to increase with later spectral types is quite obvious. Even from a cautious point of view one may read from Figure 4 that $I \approx 1.1$ for O stars and $I \approx 2$ for B stars. It should be kept in mind that these empirical results depend on the validity of the UV mass-loss rates. If, for some reason, the UV rates should turn out to be systematically wrong this would of course affect our results found for the velocity law.

Using Figure 2, I can be converted into β which turns out to be ~ 0.7 for O stars. This β value is rather insensitive to v_0/v_{∞} . We have $v_0/v_{\infty} \approx 0.01$ to a good approximation for O stars. Moreover, if $\beta < 1$ then I is nearly independent of v_0/v_{∞} . This situation reverses for B stars, however, so that one can only say β is of the order of 2–3 for B stars.

$\beta \approx 0.7$ for O stars compares quite well with the results of the mass-loss theory which predicts $\beta \sim 0.8$ (Pauldrach, Puls, and Kudritzki 1986). The results presented here are also in (at least qualitative) agreement with $v(r)$ determinations from IR data. Studies by Leitherer *et al.* (1982), Abbott, Telesco, and Wolff (1984), and Bertout *et al.* (1985) gave evidence for an

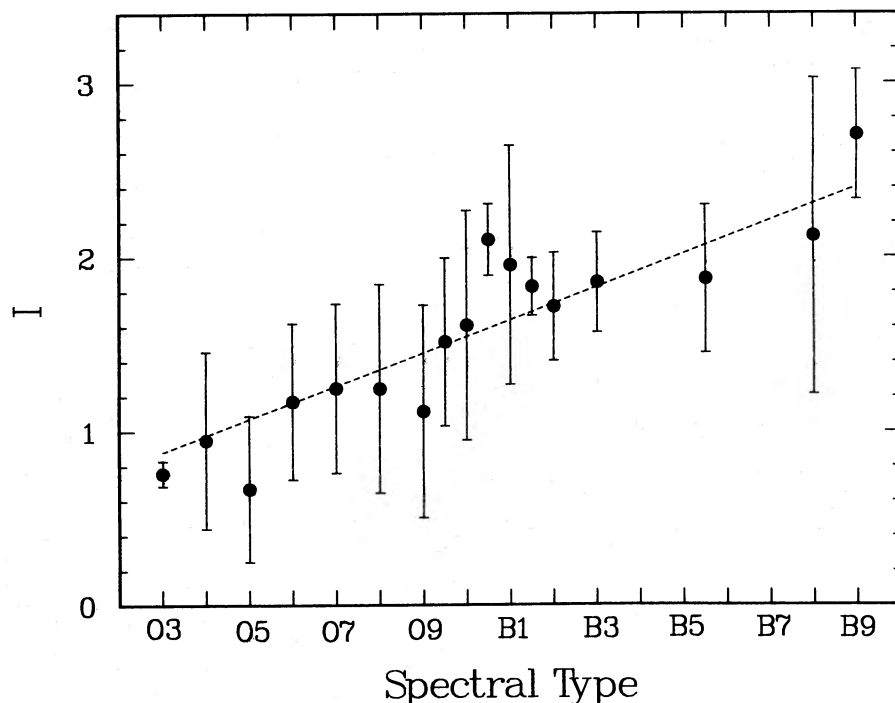


FIG. 4.—Dependence of the $v(r)$ -sensitive quantity I on spectral type

increase of β toward later spectral type with β around 1 for O stars.

We conclude that $H\alpha$ data are in agreement with results obtained from radio and UV measurements if the run of the wind velocity is explicitly taken into account. The average velocity law for O stars is somewhat shallower than the original velocity law proposed by Castor, Abbott, and Klein (1975, $\beta = 0.5$). There is a trend for the velocity law to become even shallower for later spectral types.

V. DERIVATION OF MASS-LOSS RATES

The correlation found between I and spectral type allows us to use equation (8) for determining mass-loss rates. We adopt the I versus spectral type relationship of Figure 4. This assumes the scatter of the individual points in this figure is mainly due to the use of the statistical mass-loss rate rather than a dependence of I on some other stellar parameter. We can justify this procedure *a posteriori* by comparing the mass-loss rates thus derived with the statistical rates. The former are in better agreement with radio values, which are believed to represent the "true" rates, than the statistical \dot{M} values (see the discussion below). The resulting mass-loss rates are listed in the tenth column of Table 1.

A fundamental assumption inherent in equation (8) is $\tau(H\alpha) \ll 1$. It is worthwhile to investigate the validity of this assumption for each program star. The optical depth of $H\alpha$ in the Sobolev theory is related to the velocity at distance r and the population densities of the second and third level of H by (Castor 1970):

$$\tau(H\alpha) = \frac{\pi e^2}{m_e c} (gf\lambda)_{23} \frac{r}{v(r)} \left(\frac{N_2}{g_2} - \frac{N_3}{g_3} \right). \quad (10)$$

This expression for $\tau(H\alpha)$ holds as long as $v(r)$ is higher than the thermal velocity in the flow. A representative estimate for the optical depth of $H\alpha$ can be obtained at a distance $r = 1.5 R$. The point is sufficiently far out in the wind to give $v(r) > v_{\text{thermal}}$ for typical velocity laws but is still fairly close to the star that most of the $H\alpha$ emission is sampled by the line of sight.

Equation (10) can be rewritten to give a relation of the type

$$\tau(H\alpha) \approx f(T_{\text{eff}}) \frac{\dot{M}^2}{v(r)^3 R^3}. \quad (11)$$

$f(T_{\text{eff}})$ is a temperature-sensitive factor introduced by the Saha equation. It is treated analogous to $c(T_{\text{eff}})$ in § II and varies by about a factor of 400 over a temperature range of 50,000 through 10,000 K. $\tau(H\alpha)$ can then be calculated for each star by using the stellar radius, the mass-loss rate and the corresponding β value. The eleventh column of Table 1 gives the results for the logarithm of τ . Although these numbers should serve as an estimate only, several conclusions can be drawn. O stars are optically thin in $H\alpha$ even for the most extreme cases known. The maximum value is found for HD 152408 with $\tau(H\alpha) \approx 0.05$ and typical values for O stars are between 10^{-2} and 10^{-3} . B stars generally have somewhat higher optical depth in $H\alpha$ but fulfill the condition of $\tau(H\alpha) \ll 1$ to a good approximation. This behavior can be understood from equation (11). While $f(T_{\text{eff}})$ strongly increases toward lower temperatures, this effect is largely compensated for by a decrease of the $\dot{M}^2/[v(r)R]^3$ factor. However, this no longer holds in the case of certain B hypergiants. In fact, all B hypergiants of our sample have $\tau(H\alpha) > 1$ indicating a breakdown of the \dot{M} versus $L(H\alpha)$ relation. $\tau(H\alpha)$ for HD 152236, HD 169454, HD 190603, and HD

193237 has been obtained from the observed mass-loss rates and an assumed β of 1.5. Even if the calculated optical depths are a rough guideline only, it is obvious that no mass-loss rates may be derived from the simple $H\alpha$ -equivalent method. Rather, these stars require detailed modeling of the radiative transfer in their wind. No entry is therefore given for \dot{M} of these objects in Table 1.

Cyg OB2 no. 12 was also eliminated from the original sample. Radio observations by White and Becker (1983) suggest the wind of this star has a much lower electron temperature than expected from the stellar T_{eff} . A further difficulty arises from the terminal velocity of the wind which appears to be abnormally high possibly hinting at a peculiar velocity law. In view of these uncertainties we do not derive \dot{M} for Cyg OB2 no. 12.

Figure 5 is a plot of the determined mass-loss rates versus bolometric luminosity. \dot{M} scales with L with a power of 1.6 as expected from our calibration via equation (9). Part of the scatter in this figure is due to the observational errors which become more pronounced toward lower mass-loss rates (and correspondingly lower $H\alpha$ emission-line strength). However, even if observational errors were negligible we expect a certain amount of broadening of the \dot{M}/L relation. The radiation-pressure-driven wind theory predicts an additional dependence of \dot{M} on the evolutionary state of the star. Kudritzki, Pauldrach, and Puls (1987) published evolutionary tracks in the \dot{M}/L diagram for various initial masses. These tracks define a band in this diagram and are included in Figure 5. There is reasonable agreement between these tracks and the mass-loss rates derived from $H\alpha$.

A further test of the reliability of $H\alpha$ as a mass-loss tracer is provided by a comparison of \dot{M} derived from $H\alpha$ and the UV for individual stars. Thirty-three stars of Table 1 have \dot{M} also determined by the UV method. Most of these rates are listed by Conti (1988). Figure 6 compares these UV rates with the $H\alpha$ rates derived here. There is no systematic difference between these data sets and the agreement between individual stars is better than a factor of 4 in all but one case. HD 35619 is discrepant in that it has a very low UV rate ($\log \dot{M} = -7.3$) which is much lower than expected from its luminosity. Possibly it is the UV rate and not the $H\alpha$ rate which is erroneous for this star.

The mass-loss domain where the $H\alpha$ and the UV method work best are not coincident: $H\alpha$ is most reliable for high-density winds where the underlying photospheric absorption is only a small correction [provided $\tau(H\alpha) \ll 1$ holds]. Under these conditions, UV resonance lines tend to be saturated and are only weakly sensitive to \dot{M} so that this method becomes unreliable. On the other hand, radio fluxes are most favorably detected from high-density winds. Since radio mass-loss rates are quite model-independent, they provide an important constraint on the accuracy of the $H\alpha$ rates.

Table 2 summarizes the radio data found for our sample of stars (13 objects). Stars with a possible nonthermal contribution to the radio flux have been excluded (HD 15558, HD 164794, Cyg OB2 no. 8A) or have been corrected for this effect (Cyg OB2 no. 9). The stars in Table 2 cover the spectral types O3 through B1. Obviously, the agreement between the \dot{M} values derived from radio and $H\alpha$ is excellent. There is no one star disagreeing by more than a factor of 1.8. Excluding the upper-limit entries of $\log \dot{M}(\text{radio})$ we find for the difference between $\log \dot{M}(H\alpha)$ and $\log \dot{M}(\text{radio})$ a value of 0.00 with a standard deviation of 0.17. The difference between the sta-

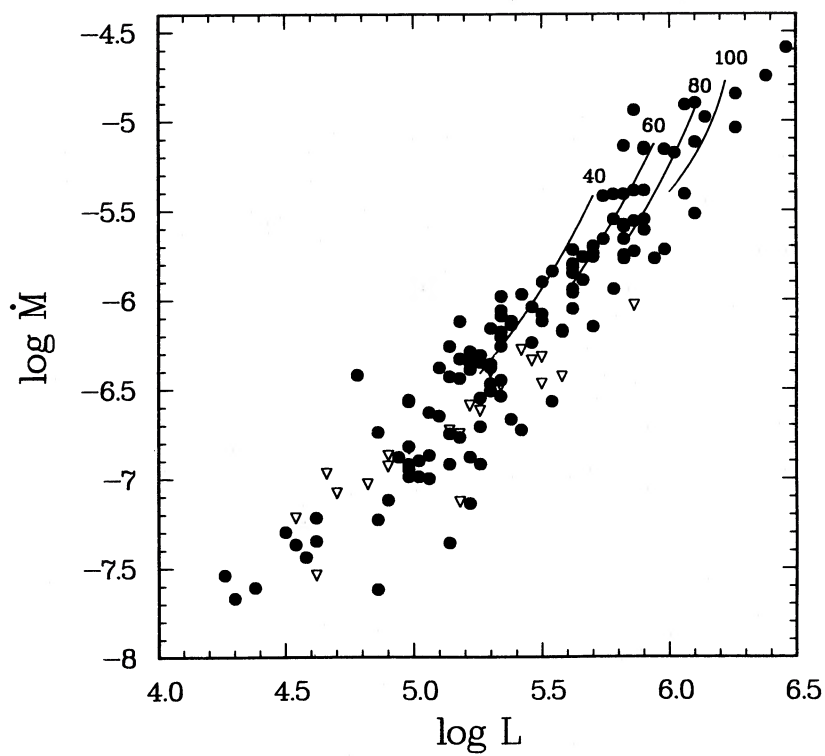


FIG. 5.—Derived $H\alpha$ mass-loss rates vs. bolometric luminosity. They are compared with theoretical tracks for initial masses $40 M_{\odot}$, $60 M_{\odot}$, $80 M_{\odot}$, and $100 M_{\odot}$.

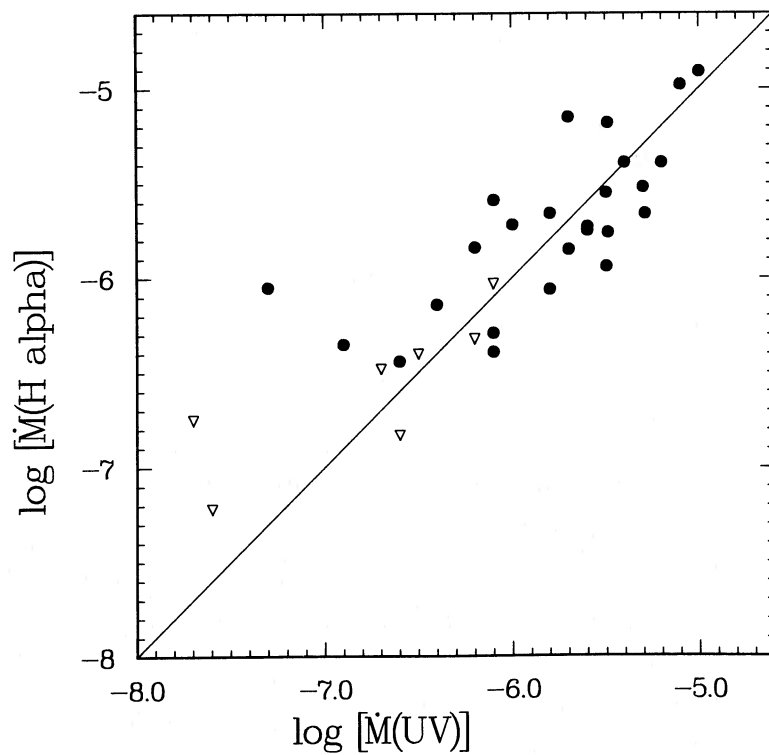


FIG. 6.—Comparison of $H\alpha$ mass-loss rates with UV mass-loss rates

TABLE 2
COMPARISON OF H α AND RADIO MASS-LOSS RATES

Object	log \dot{M} (H α)	log \dot{M} (radio)	Radio Reference
HD 2905	-5.90	≤ -5.44	1
HD 14947	-5.16	< -4.62	2
HD 15570	-4.85	-5.00	3
HD 37128	-5.76	-5.51	3
HD 37742	-5.66	-5.64	3
HD 38771	-6.04	-5.96	2
HD 66811	-5.18	-5.42	3
HD 151804	-4.98	-5.03	3
HD 152408	-4.91	-4.74	3
HD 190429A	-4.90	< 4.68	2
HD 210839	-5.39	≤ -5.30	1, 4
Cyg OB2 no. 7 ...	-5.12	≤ -4.72	1, 3, 4
Cyg OB2 no. 9 ...	-4.75	-4.72	3

REFERENCES.—(1) Abbott, Telesco, and Wolff 1984; (2) Abbott *et al.* 1980; (3) Abbott 1985; (4) Abbott, Bieging, and Churchwell 1981.

tistical \dot{M} of equation (9) and log \dot{M} (radio) is -0.01 ± 0.23 . If we take the radio value as the "correct" rate this implies that we actually improved \dot{M} as resulting from equation (8) when we replaced the statistical \dot{M} by the mass-loss rate following from the I versus spectral type relation. (See the beginning of this section.)

We emphasize that we are dealing with small-number statistics and that the perfect agreement of Table 2 may be fortuitous. In view of the possible error sources we do not expect H α to agree with the radio by the above factor of 1.8. D. C. Abbott (1987, private communication) found evidence for an overabundance of processed material in the winds of evolved O stars. This implies that the derived radio mass-loss rates

might be somewhat too low. However, it has become evident from the previous discussion that there is no systematic difference between mass-loss rates derived from H α and other methods. Furthermore, the typical accuracy of an H α mass-loss rate is of the order of a factor of 3 or better which is comparable to the accuracy of the UV method.

As an interesting by-product of this study we found that \dot{M} for early- and mid-O stars derived from the original KC formulae are on the average in quite good agreement with radio and UV data. KC adopted a steep velocity law with $\beta \approx 0.5$ which tends to overestimate \dot{M} but also used a terminal velocity of ~ 1500 km s $^{-1}$ that underestimates \dot{M} . Since we derive $\beta \approx 0.7$ for early- to mid-O stars which typically have $v_\infty \approx 3000$ km s $^{-1}$, this implies that the two errors in KC should approximately cancel. Figure 7 supports this expectation. In this figure we compare \dot{M} derived from the KC formulae for O and B stars with the prediction of equation (9). On the average, \dot{M} for O stars is in agreement with equation (9) due to the expected effect of the counteracting error sources canceling each other. In contrast, \dot{M} for B stars disagrees with equation (9). The terminal velocities in B stars are closer to those which KC adopted and the B star velocity law is even more gradual than the O star law. Consequently, \dot{M} of B stars is overestimated when using the KC formulae. (It should be noted that the KC computations were never intended to be applied to B stars.)

These results suggest that mass-loss rates derived from the KC calculations published for early- and mid-O stars are basically correct. This is in contradiction to what is usually claimed in the literature, namely H α generally overestimates \dot{M} . Lamers (1981) found that H α mass-loss rates are too high by 0.27 ± 0.11 in log \dot{M} on the basis of the three comparison stars HD 14947, HD 37742, and HD 66811. It turns out, however,

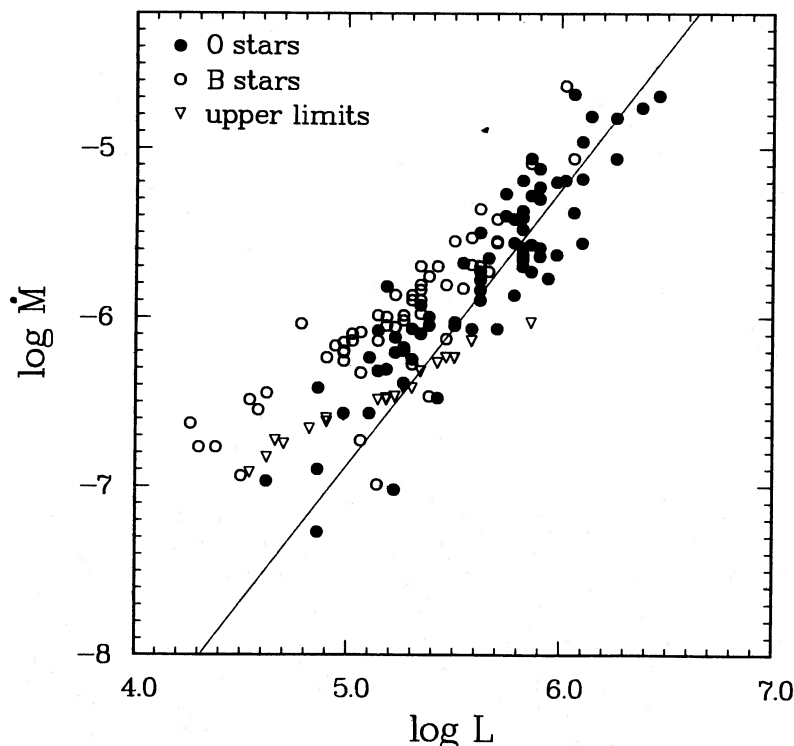


FIG. 7.—Mass-loss rates derived from the KC formulae for O and B stars. The solid line represents the prediction of eq. (9)

that his results are mainly a result of small-number statistics. HD 14947 (O5 If) and HD 66811 (O4f) are somewhat exceptional in that they have $H\alpha$ mass-loss rates higher by about a factor of 2 than the statistical and/or the radio rates. HD 37742 is in excellent agreement with radio data but only if $v(r)$ is accounted for in this O9.7 star. As a consequence, these three stars happen to have higher than average mass-loss rates when derived via KC.

VI. CONCLUSIONS

The observed equivalent width of $H\alpha$ in OB stars provides a simple but accurate way to determine the mass-loss rates in these stars. Since $H\alpha$ originates in a wind region close to the star where the flow is still accelerating, this method requires the knowledge of the velocity law. It has been shown in the present paper that the $v(r)$ influence on the $H\alpha$ luminosity can be accounted for by adopting a dependence of $v(r)$ on spectral type. Even if the actual velocity law may somewhat vary from star to star, this procedure allows one to derive mass-loss rates which are not inferior to UV rates of galactic stars. However, one should keep in mind that the results found in this paper depend on the adopted UV calibration. Systematic differences between UV and $H\alpha$ may still exist but they are not detectable by the method followed in this study. This is even more true in the case of the B stars, where the velocity law has been derived from an extrapolation of equation (8).

The value of the $H\alpha$ method may even increase as soon as further observational and theoretical constraints exist which can narrow down the possible range for the velocity law of a given star. In this case, $H\alpha$ will be a rather model-independent mass-loss tracer, in contrast to the UV method which has to make assumptions about the ionization structure and the chemical composition of the envelope.

$H\alpha$ can provide an important diagnostic of mass loss from extragalactic OB stars. No mass-loss rates for normal extragalactic OB stars have been published to date. Even the closest

extragalactic stars in the LMC and the SMC are too faint to measure their radio flux or to obtain *IUE* high-resolution spectra in reasonably short integration times. *IUE* low-resolution spectra have been obtained, but it is difficult to derive \dot{M} from these data as can be seen from the results of Garmany and Conti (1985). Since $H\alpha$ equivalent widths can be measured even with moderate spectroscopic resolution, this method is capable of deriving \dot{M} for many luminous OB stars in the Local Group. The required information on v_∞ can be obtained from *IUE* low-resolution spectra in the case of LMC and SMC stars. In addition, long-exposed *IUE* high-resolution spectra for a few LMC/SMC OB stars are extremely useful. They can serve as an empirical test of whether the $H\alpha$ method works as well in these galaxies until there are theoretical models of $H\alpha$ line formation in metal-deficient stars.

The theory of radiation-pressure-driven winds predicts a dependence of \dot{M} on metallicity. Kudritzki, Pauldrach, and Puls (1987) find $\dot{M} \approx Z^{0.5}$. Accordingly, \dot{M} in the SMC should be lower by a factor of 3 as compared with the Galaxy. If this prediction proves to be true, significant consequences for the evolution of the massive star population are to be expected. However, as shown by Kudritzki *et al.*, the mass-loss rate actually observed may critically depend on the evolutionary state of the star. The metallicity effect on \dot{M} for a star will then be hidden by the improper knowledge of the stellar parameters. This obstacle can be overcome by improving statistics, i.e., observing a large number of stars. This again favors the $H\alpha$ method which is able to provide mass-loss rates for many extragalactic stars with a moderate amount of observing time.

Stimulating discussions with David Abbott, Peter Conti, Katy Garmany, and David Hummer are gratefully acknowledged. I am grateful to John Castor for useful correspondence. This work has been supported by a Feodor-Lynen Fellowship of the Alexander von Humboldt Foundation and by NSF grant AST 85-20728 through the University of Colorado.

REFERENCES

- Abbott, D. C. 1978, *Ap. J.*, **225**, 893.
 ———. 1982, *Ap. J.*, **259**, 282.
 ———. 1985, in *Radio Stars*, ed. R. M. Hjellming and D. M. Gibson (Dordrecht: Reidel), p. 61.
 Abbott, D. C., Biegging, J. H., and Churchwell, E. 1981, *Ap. J.*, **250**, 645.
 Abbott, D. C., Biegging, J. H., Churchwell, E., and Cassinelli, J. P. 1980, *Ap. J.*, **238**, 196.
 Abbott, D. C., Telesco, C. M., and Wolff, S. C. 1984, *Ap. J.*, **279**, 225.
 Auer, L. H., and Mihalas, D. 1972, *Ap. J. Suppl.*, **24**, 193.
 Bertout, C., Leitherer, C., Stahl, O., and Wolf, B. 1985, *Astr. Ap.*, **144**, 87.
 Burki, G., and Llorente de Andr s, F. 1979, *Astr. Ap.*, **70**, L13.
 Burki, G., Heck, A., Bianchi, L., and Cassatella, A. 1982, *Astr. Ap.*, **107**, 205.
 Castor, J. I. 1970, *M.N.R.A.S.*, **149**, 111.
 Castor, J. I., Abbott, D. C., and Klein, R. I. 1975, *Ap. J.*, **195**, 157.
 Castor, J. I., and Lamers, H. J. G. L. M. 1979, *Ap. J. Suppl.*, **39**, 481.
 Conti, P. S. 1974, *Ap. J.*, **187**, 539.
 ———. 1988, in *O, Of and Wolf-Rayet Stars*, ed. P. S. Conti and A. Underhill (NASA/CNRS Monograph), in press.
 Conti, P. S., and Frost, S. A. 1977, *Ap. J.*, **212**, 728.
 Conti, P. S., and Garmany, G. D. 1980, *Ap. J.*, **238**, 190.
 Ebbets, D. 1982, *Ap. J. Suppl.*, **48**, 399.
 Garmany, C. D., and Conti, P. S. 1984, *Ap. J.*, **284**, 705.
 ———. 1985, *Ap. J.*, **293**, 407.
 Garmany, C. D., Olson, G. L., Conti, P. S., and Van Steenberg, M. E. 1981, *Ap. J.*, **250**, 660.
 Gathier, R., Lamers, H. J. G. L. M., and Snow, T. P. 1981, *Ap. J.*, **247**, 173.
 Humphreys, R. M. 1978, *Ap. J. Suppl.*, **38**, 309.
 Hutchings, J. B., and von Rudloff, I. R. 1980, *Ap. J.*, **238**, 909.
 Klein, R. I., and Castor, J. I. 1978, *Ap. J.*, **220**, 902 (KC).
 Kudritzki, R. P., Pauldrach, A., and Puls, J. 1987, *Astr. Ap.*, **173**, 293.
 Kurucz, R. L. 1979, *Ap. J. Suppl.*, **40**, 1.
 Lamers, H. J. G. L. M. 1981, *Ap. J.*, **245**, 593.
 Leitherer, C., Hefele, H., Stahl, O., and Wolf, B. 1982, *Astr. Ap.*, **108**, 102.
 Leitherer, C., *et al.* 1987, *Astr. Ap.*, in press.
 Maeder, A. 1984, in *IAU Symposium 105, Observational Tests of Stellar Evolution Theory*, ed. A. Maeder and A. Renzini (Dordrecht: Reidel), p. 299.
 Mihalas, D. 1972, NLTE Atmospheres of B and O Stars (NCAR TN/STR-76).
 Olson, G. L., and Ebbets, D. 1981, *Ap. J.*, **248**, 1021.
 Peppel, U. 1984, *Astr. Ap. Suppl.*, **57**, 107.
 Pauldrach, A., Puls, J., and Kudritzki, R. P. 1986, *Astr. Ap.*, **164**, 86.
 Rosendhal, J. D. 1973, *Ap. J.*, **186**, 909.
 Sterken, C., and Wolf, B. 1978, *Astr. Ap.*, **70**, 641.
 Schmidt-Kaler, T. 1982, in *Landolt-Bornstein, New Series, Group VI, Vol. 26*, ed. K. Schaifers and H. H. Voigt (Berlin: Springer-Verlag), pp. 1 and 449.
 White, R. L., and Becker, R. H. 1983, *Ap. J. (Letters)*, **272**, L19.

CLAUS LEITHERER: Joint Institute for Laboratory Astrophysics, University of Colorado, Boulder, CO 80309-0440